Nanobubbles effect on the mechanical flotation of phosphate ore fine particles

Ziaeddin Pourkarimi [1], Bahram Rezai [1], Mohammad Noaparast [1,2]

[1] Department of Mining and Metallurgical Engineering, Amirkabir University of Technology (Tehran Polytechnics), Tehran, Iran.

[2] School of Mining Engineering, University of Tehran, Tehran, Iran

Corresponding author: rezai@aut.ac.ir (Bahram Rezai)

Abstract: Froth flotation is one of the main methods for processing of phosphate ores. However, flotation of fine particles, especially phosphate ores, has always been one of the fundamental problems. For example, about 10% of Esfordi phosphate processing plant ore with a grade of more than 16% P_2O_5 and d_{80} of less than 30 µm is sent to the tailing dam. Flotation using nanobubbles generated by hydrodynamic cavitation is one of the latest industrial techniques to recycle fine particles of minerals. A significant recovery increment in flotation of fine particles using nanobubbles has been one of the main topics of flotation science in recent years. Fine bubbles have important effects on the gas holdup, which is necessary in the froth flotation cell of mineral based process industries. At a given gas holdup, using finer bubbles can reduce frother consumption. An exclusive nanobubble generation system has been developed at Iran Mineral Processing Research Center (IMPRC) for evaluating the effect of nanobubbles on froth flotation. This device enhances venturi tubes and works based on cavitation phenomena. In this study, a comparison of conventional flotation and nanobubble enhanced flotation in mechanical cells was carried out on two types of phosphate ore samples. As a result, the flotation recovery had a significant increment of more than 30% in the case of using nanobubbles versus conventional flotation in the same grade of P_2O_5.

1. Introduction

Decreasing the high grade mineral resources with a simple mineral composition and achieving low grade deposits with complex compounds impose more grinding to reach the releasing degree of minerals. Furthermore, in mining operations such as exploitation, transportation and comminution, a part of the ore that contains valuable material, is converted to fine particles. The presence of fine particles in the flotation environment, not only causes a decrease in the process efficiency, but also causes an increase in the reagent consumption. According to most mineral processing references, fine particles are usually particles smaller than 38 µm in general as well as ultrafine particles which are less than 13 µm (Ahmadi and Khodadadi Darban, 2013). The problem of processing fine and ultrafine mineral particles by flotation continues to be one of the major technical challenges in the area of mineral processing (Sivamohan, 1990). Some agreement exists in that the problem is caused by the inherent properties of these particles: small mass, high interfacial free energy, etc. Thus, the main flotation drawbacks are related to the low probability of bubble-particle collision and adhesion, mechanical entrainment and entrapment, slime coating, higher flotation reagent adsorption, formation of dense froths and low process kinetics.

The processing of fine particles has been started from many years ago. Gaudin (1942) proposed that the rate of flotation was independent of particle diameter up to 4 µm and proportional to the diameter for particles in the range of 4–20 µm (Miettinen et al., 2010).

The first theoretical model to describe collision between a fine particle and a bubble was developed by Sutherland (1948). He proposed that the rate of flotation could be found by assuming that the flow around the bubble was the uniform motion of an inviscid fluid. Thus, the streamlines around the bubble could be calculated using a potential flow theory. Assuming that particles have no influence on the flow field, bubble–particle collision occurs when the particle lies on a streamline which brings it within one particle radius of the spherical bubble surface (Miettinen et al., 2010).

In 1961, Derjaguin and Dukhin produced a key paper on fine particle flotation dealing with the theory of flotation of small and medium-sized particles. Derjaguin and Dukhin (1961) formally proposed that the overall rate of flotation is equal to the product of three probabilities or efficiencies: bubble– particle collision, attachment and stability (Miettinen et al., 2010).

Reay and Ratcliff (1973) suggested that two flotation regimes might exist. They proposed that the first regime occurs for particles with diameters greater than 3 μm, where the bubble–particle collision efficiency increases with increasing particle size. For particles with a diameter less than several micrometers, they become susceptible to Brownian diffusion and enter a second flotation regime. Brownian diffusion is the main collision mechanism operative when particles approach molecular dimensions. Diffusion is an effective mass transfer mechanism, and the loss of inertia associated with fine particles becomes a positive advantage in Brownian motion. Therefore, one would expect the bubble–particle collision efficiency to increase with a reduction in particle size in the diffusion regime (Miettinen et al., 2010).

In 1977, Anfruns and Kitchener published the first measurements of the collection efficiency between fine particles and bubbles under potential flow conditions. This was the first critical test of Sutherland's collision theory under conditions where the particle and bubble surface chemistry was controlled (Miettinen et al., 2010).

The data of Nguyen et al. (2006) showed that bubble–particle collection efficiency is a minimum at a particle size around 100 nm or 0.1 μm. With larger particles, the interception and collision mechanisms apparently dominate, while the diffusion and colloidal forces control the collection of particles with a size smaller than the detected transition size of 100 nm (Miettinen et al., 2010). Hampton and Nguyen (2010) also found that the effect of nanobubbles on flotation of coal in saline environments is important due to the changes on the surface characteristics of the mineral species.

In recent years, the processing of fine particles has been studied from different aspects, and new methods in order to recover the fines have been also provided. Methods such as centrifugal flotation (Colic, et. al. 2007), agglomeration-flotation (Sadowski and Polowczyk, 2004), floc-flotation (Tasdemir, et. al., 2011), electro-flotation (Kaisar Alam, 2012), DAF or dissolved air flotation (Rodrigues and Rubio, 2007) or Jameson flotation methods (Mohanty and Honaker, 1999; Tasdemir, et. al., 2007), etc. have been proposed to increase the rate of fine particle flotation. One of these methods, which has been developed during recent years, is flotation in the presence of nanobubbles generated by hydrodynamic cavitation, which is used simultaneously with conventional bubbles. Fan and Tao (2008) applied this technique for flotation of large and ultrafine particles of coal and phosphate. Furthermore, Sobhy and Tao (2013) used nanobubbles in flotation of fine particles of coal. Ahmadi and Khodadadi Darban (2013) developed nanobubbles for flotation of fine particles of pure chalcopyrite. Also recently, Zhang and Seddon (2016) have focused on interactions of nanobubble and gold nanoparticles in bulk solutions. They found that unlike froth flotation, where bubble–particle interactions are driven mainly through collisions, for bulk nanobubble solutions the principle interaction is through nucleation of new nanobubbles on the particles.

In addition, many mineral processing plants have lost their fine particles various stages of processing. Esfordi phosphate processing plant, which is located in Yazd province of Iran, with the capacity of 50 Mg/h P_2O_5 lost more than 10% of its ore, as particles smaller than 38 μm, in crushers dedusting systems and desliming cyclones before flotation. These particles, in addition to having high-grade phosphate, also have high rates of rare earth elements. Furthermore, because of their very small size, they have actually reached a releasing degree (Shafaei, 2006). Directing researches towards finding specific methods for the processing these types of minerals could be very economical. Hence, the aim of this study was to investigate the mechanisms of phosphate fines flotation in the presence of nanobubbles which are generated by hydrodynamic cavitation.

2. Materials and methods

This study was performed on fine particles of Esfordi phosphate processing plant from the central desert of Iran in Yazd province. Hydrodynamic cavitation was used for generation of nanobubbles. Cavitation, which has different types, is the formation and simultaneous collapse of vapor cavities in a liquid. It usually occurs when a liquid is subjected to rapid changes of pressure that cause the formation of cavities where the pressure is relatively low. When subjected to higher pressure, the voids implode and can generate an intense shock wave (Zhou et al., 1994; 2009). This study has particularly focused on hydrodynamic cavitation. Hydrodynamic cavitation describes the process of vaporization, bubble generation and bubble implosion, which occur in a flowing liquid as a result of a decrease and subsequent increase in the local pressure.

The generation of nanobubbles was carried out based on cavitation phenomenon through venturi tube. For this purpose, a particular device which was produced and developed at IMPRC (Iran Mineral Processing Research Center) was applied. The schematic setup of the nanobubble generating and sampling system to measure the bubble size and volume is presented in Fig. 1. Online measurement of the bubbles size was implemented by Laser Particle Size Analyzer (LPSA) according to standard BS ISO 13320_09. The Malvern mastersizer 2000 LPSA was used for measuring the size distribution and volume of bubbles as well (Pourkarimi, 2017).

As shown in Fig. 1, the identified frother could be added into the conditioning tank and after appropriate conditioning time, the solution is sent to the venturi tube among static mixers, due to the suction, which results from the centrifugal pump. The point where the velocity of stream declines and the pressure suddenly increases results in the hydrodynamic cavitation phenomena which leads to nanobubble generation. The venturi tube inlet pressure of the solution as well as compressed air flow is adjustable. The compressed air or specified gas can be added to the solution before entering the pump. The solution containing nanobubbles is transferred to the laser particle size analyzer through pump propulsion for online measurement of bubble size. Then, the solution which contains nanobubbles could be added to the mechanical flotation cell. The effect of nanobubbles on the fine particles to attach to conventional bubbles can be observed in Fig. 1 (Pourkarimi, 2017).
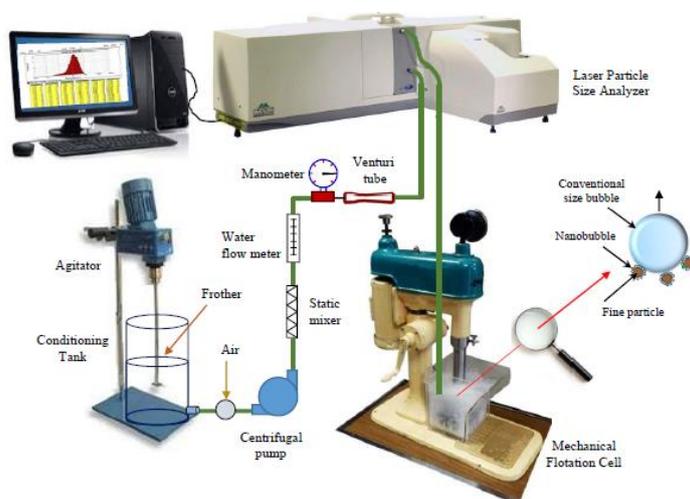
Fig. 1. Schematic setup of nanobubble generator for flotation of fine particles and laser particle size analyzer online measurement system (Pourkarimi et al., 2017)

The advantage of the cavitation venturi tube-generated picobubbles and nanobubbles, incorporated with conventional-sized bubbles such as micro-bubbles in flotation, has been explained by two factors that contribute to the increased flotation rate constant: *i*) picobubbles and nanobubbles formed in situ on hydrophobic particle surfaces may cause aggregation by a bubble-bridging mechanism, resulting in increased collision probability with the bubbles; *ii*) particles frosted with pico-nanobubbles may present a surface favorable for attachment to conventional flotation sized bubbles (Tao, 2004; Zhou et al., 2009).

2.1 Flotation

First of all, for performing flotation tests, a certain amount of frother, using a digital scale with 5 decimal places of accuracy was weighed and added to the 15 dm³ conditioning tank of the nanobubble generator device (Fig. 1). After 5 min of mixing, the frother was solved. In the following, some amount of the ore (based on various solid content) along with water in a 1.5 dm³ mechanical flotation cell was mixed. The slurry pH, was adjusted to 9.5 (operating pH in the plant) using NaOH. In addition, starch was used for inhibiting the iron oxides. After the initial conditioning, Flo-Y-S, which is a type of fatty acid, was applied as a collector with the identified concentration and proper conditioning time. Flo-Y-S selectively effects on the surface of phosphate particles, and let them to be floated. The optimized concentration of the collector and inhibitor was equal to 500 g/Mg and 400 g/Mg, respectively for conventional flotation in the absence of nanobubbles. Also, considering the optimum point of grade and recovery, the proper time for initial and collector conditioning was 5 and 3 min, respectively. Also, aeration and frothing time was 1 and 3 min, respectively.

Since the experiments were carried out in both the presence and absence of nanobubbles, the manner of adding the frother was different. In order to inject the nanobubbles into the flotation process, considering continuity of the process of nanobubble generation, it could not to be stopped. Therefore, the intended volume of nanobubble solution could be adjusted with the flow control with the duration of time. The flow of adding nanobubbles in all of the experiments was equal to 2000 cm³/min. After 1 min of adding the frother, the air valve would be opened. The aeration rate of the flotation cell and nanobubble generator in all of the test works (except where noted) were 500 and 200 cm³/min. The froth height from the edge of the cell was about 10 mm. The frothing process was manual and performed every 10 sec. It was continued up to 3 min and the flotation concentrate and tailing were filtered and dried separately. The samples were analyzed for P_2O_5 and Fe content by ICP-OES and wet chemistry, respectively.

Fig. 2 shows the effect of frother type and concentration on the bubble size. Clearly, it could be found that Flo-Y-S, which is a type of fatty acid, comparing to MIBC, generated finer bubbles using lower amounts of reagent (Pourkarimi, et al., 2017).
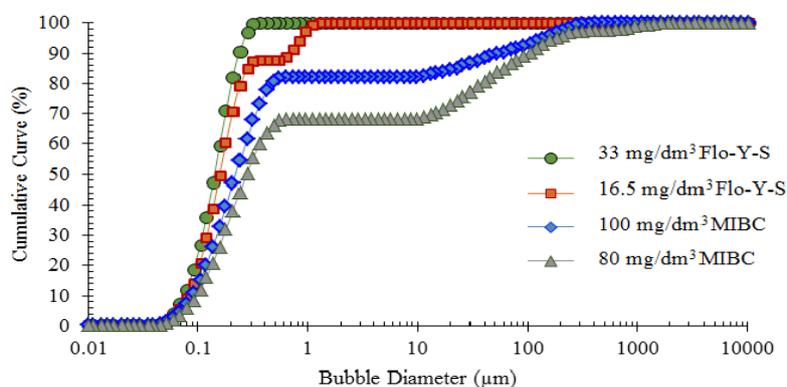
Fig. 2. Effect of frother concentration on bubble size, comparison of MIBC and Flo-Y-S (Pourkarimi et al., 2017)

2.2 Materials

2.2.1 Sampling

In order to perform flotation tests on phosphate fine particles, the sample was prepared from Esfordi phosphate processing plant, which is located in Yazd province of Iran. The targeted samples were related to crushing section dust collectors, which had a higher grade of P_2O_5 and the other was desliming cyclones as well which was lower in grade despite its higher amounts. The total produced fine particles (-38 μm) of Esfordi plant were more than 10% of the plant capacity (Tavakoli, 2007).

Considering the importance of sampling and providing a representative sample, in addition to the variation of the run of the mine and the plant feed during time, it was necessary to gain the sample for more than three months, which was impossible because of the high amount of water that was along with the sample. Another problem, which was more important than the first, was lack of access to an

automatic sampler in the plant. Hence, due to existence of the blended deposit of the ore, which was representative of various zones of the mine, the sample was obtained from them and more than one Mg of ore was transferred to IMPRC. Two destinations similar to the plant circuit were performed to prepare the suitable sample. Finally, the size distribution and chemical properties of the obtained samples were compared with the real samples, in which much similarity was observed.

2.2.2 Sample preparation

Due to the diameter of real dusts in the crushing section of the plant which was equal to d_{100}= -38 μm, the preparation of this sample was performed with the dry screen.

In order to prepare the equivalent sample with the desliming cyclone overflow, all steps of processing were carried out similar to the plant circuit in the laboratory. Initially, the sample was crushed by jaw and cone crushers, respectively, down to -1000 μm. Afterwards, a laboratory ball mill and control screen with an aperture of 150 μm were used to produce d_{80} of 100 μm. Finally, a 38 μm screen was applied to separate fine particles by wet screening. Fig. 3 shows the flowsheet of the Esfordi processing plant. At all steps of processing and sampling the target samples could be observed as point A and B in Fig. 3, and they were called by the same names.
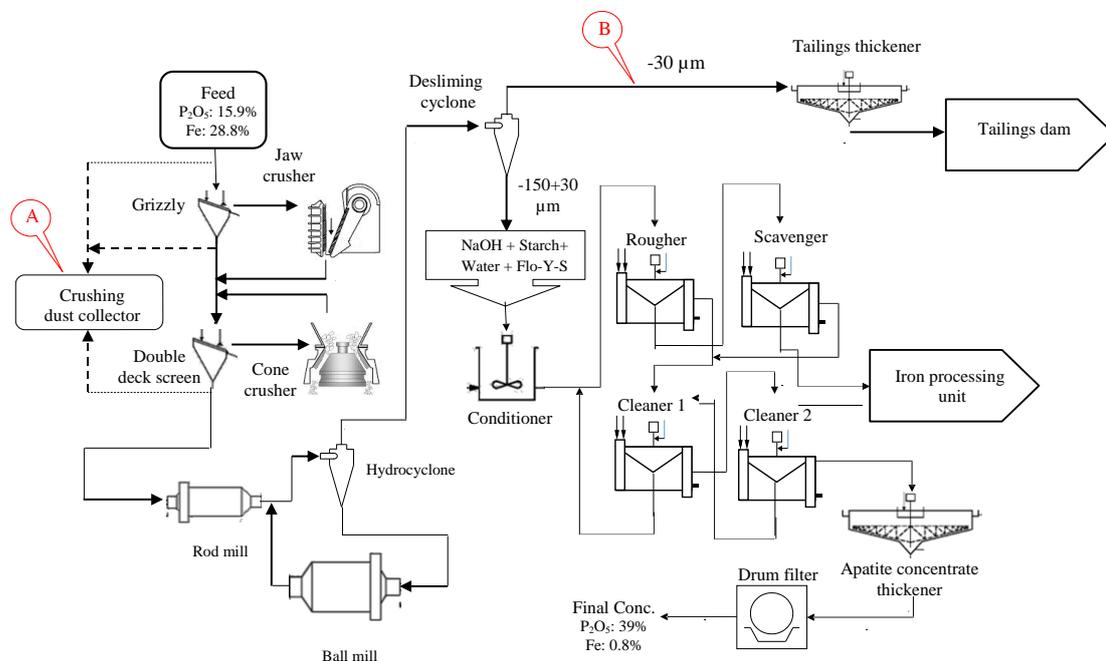
Fig. 3. Esfordi phosphate processing flowsheet (Tavakoli, 2007)

The size of the prepared samples equivalent to crushing dusts (A), and desliming cyclone overflow (B) were determined by the laser particle size analyzer (LPSA) based on standard BS ISO 13320-09. The results of this evaluation can be seen in Table 1. Clearly, it could be found that the size of two samples were the same, and smaller than 38 μm. However, the dimension of sample A was slightly coarser than sample B.

Table 1. Comparative screen analysis of equivalent and real sample

Sample/Size	Crusher dust (A)		Desliming cyclone overflow (B)	
	Equivalent sample	Esfordi real sample	Equivalent sample	Esfordi real sample
d_{10} (μm)	2.19	2.16	1.58	1.3
d_{50} (μm)	15.03	12.73	12.08	10.05
d_{90} (μm)	37.12	38.83	35.39	30.14

2.2.3 Chemical analysis

The chemical analysis of the prepared samples was performed by XRF and ICP-OES, and the results are presented in Table 2. In addition, the comparative results of chemical analysis are shown in Table 2. According to Table 2, it could be found that there were a lot of similarities between synthesized and real samples. The amount of P_2O_5, which was the target mineral in both samples A and B, was slightly lower than in the real samples. Similarly, the amount of Fe_2O_3, which was the main tailing was much more than in the real sample. This made the work more difficult. In other words, if concentration in the case of this sample was successful, it would be much easier in the actual case.

Table 2. Chemical analysis of prepared and real samples

Sample/Compound	Unit	Crusher dusts		Desliming cyclone overflow	
		Equivalent sample	Esfordi real sample	Equivalent sample	Esfordi real sample
P_2O_5	(%)	24.77	26.70	13.60	17.00
Fe_2O_3	(%)	23.49	16.0	39.03	34.10
SiO_2	(%)	5.71	7.50	16.47	14.20
CaO	(%)	34.93	37.10	20.30	25.30
MgO	(%)	3.44	4.0	3.27	1.00
K_2O	(%)	<0. 1	0.088	0.43	0.49
Al_2O_3	(%)	0.90	0.58	1.63	1.90
TiO_2	(%)	0.54	0.24	0.72	-
Ce	(ppm)	5814	4853	3532	2866
La	(ppm)	2444	1913	1460	1107
Nd	(ppm)	1938	-	1188	-

2.2.4 Mineralogy

X-Ray diffraction (XRD)

The mineralogical composition of the samples was studied by the X-Ray diffraction (XRD) method. The device used for this purpose was manufactured by Philips Co. Netherlands, model X'pert. The XRD plots of sample A and B are shown in Fig. 4. Furthermore, the semi-quantitative amounts of these two samples minerals are seen in Table 3. The minerals such as apatite and hematite were the main minerals, and quartz, calcite, talc and chlorite were detected in this ore as minor minerals. As it can be seen in Table 3, the constituent minerals were the same, but their amounts were a little different.
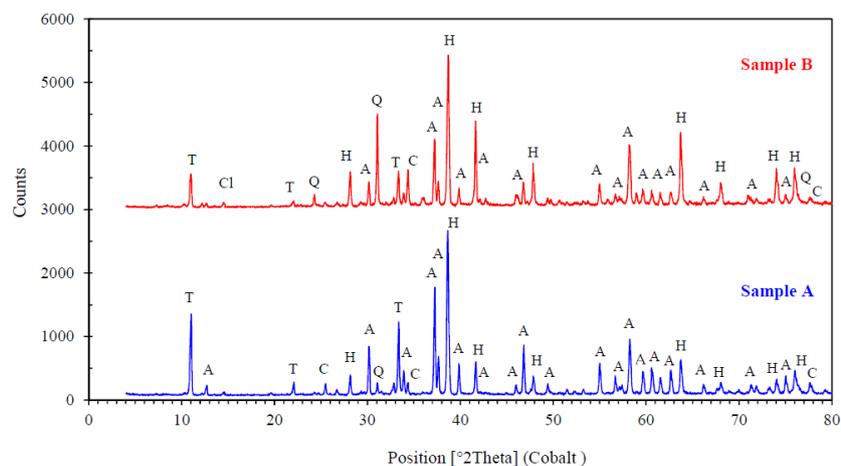
Fig. 4. XRD results of samples A and B

Table 3. XRD semi-quantitative results of samples A and B

Mineral name	Chemical formula	Symbol	Semi-quantitative amount (%)	
			Sample A	Sample B
Apatite	$Ca_{10}(PO_4)_6(OH,F,Cl)_2$	A	48	23
Hematite	Fe_2O_3	H	24	39
Calcite	$CaCO_3$	C	7	13
Quartz	SiO_2	Q	6	17
Talc	$Mg_3Si_4O_{10}(OH)_2$	T	15	6
Chlorite	$(Mg,Fe)_6(Si,Al)_4O_{10}(OH)_8$	Cl	-	2

Scanning electron microscopy (SEM)

In order to prepare the sample for SEM analysis, considering the size of the sample, Warman Cyclosizer was applied to classify the sample in 6 fractions. This device included 5 cyclones which could separate the particles by centrifugal force down to -5 μm. The mentioned fraction contained -38+33, -33+23, -23+15, -15+12, -12+5, and -5 μm. The device used for this purpose was from LEO Co., model 1450VP manufactured in England, which was equipped by EDS. In this method, the images were prepared from the sections at magnifications of ×600, ×2000, and ×5000 in various dimensions of the particles. The EDS images were taken from some unknown particles, which were conflicting with each other for more accuracy.
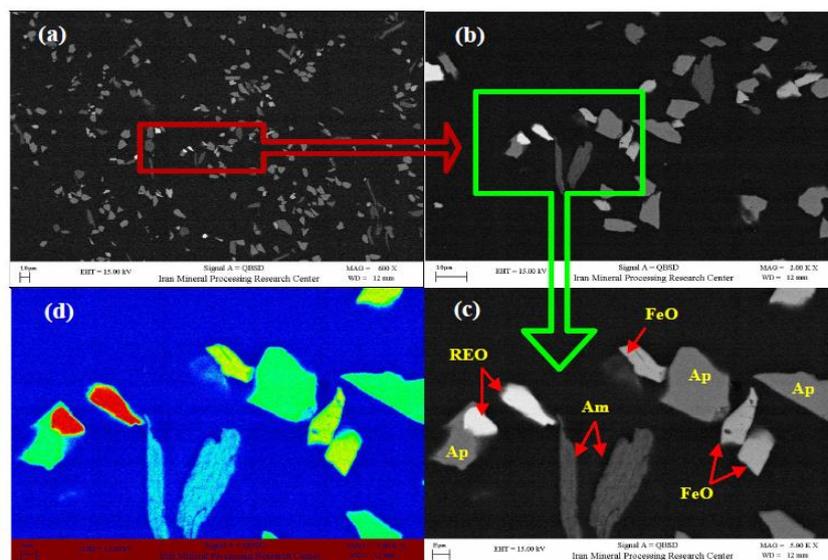
Fig. 5. BSE-Image of Esfordi phosphate sample A in fraction -12+5 μm at magnifications (a) ×600, (b) ×2000, (c) ×5000, and (d) heat map

The mineralogical studies showed that ferrous minerals such as hematite, apatite, quartz and calcite were the main mineral component, and chlorite, amphibole, illite, titanium dioxide, iron sulphide and REE-bearing minerals were secondary minerals in this sample.

Due to the fineness of the samples, the main mineral particles were mostly free, and conflicts were actually as inclusions in the main minerals, similar to the inclusion of titanium in magnetite or REE minerals within apatite, as well as triplex conflicts such as hematite-quartz-apatite. Furthermore, rare earth minerals were observed in two cases. One was inside the apatite structure, and the another was as monazite and xenotime. It is worth noting that based on the author's knowledge, the identification of the xenotime in this ore was performed for the first time through this study.

The images of the samples based on EDX-SEM from fraction of -12+5 μm is shown in Fig. 5. The variety of minerals was exhibited in this figure. Also, in order to display the difference of minerals, a heat map was applied in this picture. Hot and bright colours represent the heavier minerals and as the

color becomes darker and colder, it demonstrates that the mineral is lighter. Minerals such as apatite, hematite, monazite, xenotime and amphibole, are recognizable in Fig. 5.

3. Results and discussion

3.1 Conventional flotation experiments in the mechanical cell

Numerous flotation tests were performed on high and low grade phosphate samples in the absence of nanobubbles, and the effect of various parameters on grade and recovery of the concentrate such as solid content, frother dosage, pH of the slurry, aeration rate, frothing time, and other similar conditions were evaluated. Due to the lower grade of the desliming cyclone overflow, most of these tests were carried out on this sample. It was assumed that if the results of these experiments were positive, it could be extended to the higher grade samples (dusts).

3.1.1 Effect of collector consumption

With the aim of selecting the proper collector consumption, to produce a concentrate with suitable grade and recovery, the flotation tests were carried out with different collector dosages. These tests conditions were included, solid content 10%, pH 9.5, rotor speed 1000 rpm, inhibitor: starch (400 g/Mg), initial conditioning time 5 min, collector conditioning time 3 min, frothing time 3 min. According to the frothability of the collector, further frother was not used. The amount of collector, based on references, was intended in the range of 500-2000 g/Mg. Fig. 6 shows the variation of P_2O_5 content and recovery versus different collector dosage.
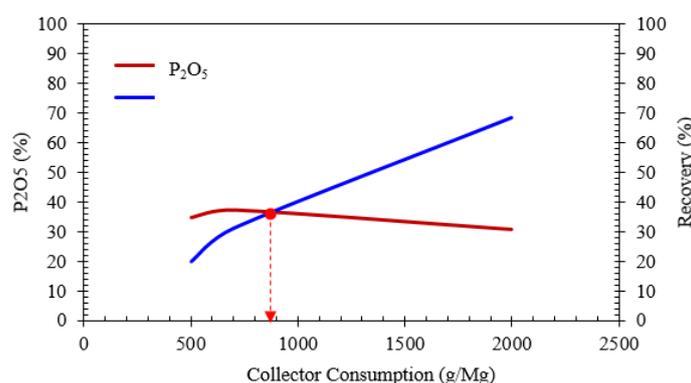
Fig. 6. Grade and recovery curve based on amount of collector

The optimal point of consumption of Flo-Y-S was determined at 870 g/Mg. The maximum grade of P_2O_5 was obtained as 700 g/Mg as well. However, in the rest of conventional flotation and flotation in the presence of nanobubbles, the consumption of 500 g/Mg was applied, to be compared and adapted with the current consumption at the Esfordi plant.

3.1.2 Effect of solid content and frother type in conventional flotation

Although the result of previous studies showed the common solid content in the flotation of fine particles was less than 10% (Fan et al., 2010d), nevertheless, in this study, the flotation tests in two solid contents of 7% and 25% were applied to ensure more. Also, these tests were performed in the presence and absence of MIBC (methyl isobutyl carbinol) as a frother with the dosage of 20 g/Mg. Sample A was used for these experiments, and the conditions were as follows: solid content: variable, rotor speed 1000 rpm, pH 9.5 which was adjusted by NaOH, inhibitor: starch (400 g/Mg), initial conditioning time 5 min, collector conditioning time 3 min, frothing time 3 min. The tests results are presented in Table 4. It was observed that the increment of solid content from 7 to 25% caused a decrease of about one percent in P_2O_5 grade. Also, the presence of MIBC reduced the grade of P_2O_5, and its absence caused a significant increase in the grade. Furthermore, in the absence of MIBC, unlike the recovery, which was increased, especially in lower solid content, the enrichment ratio was higher in lower solid contents, as well as the absence of MIBC. It is worth mentioning that although the

recovery in the presence of MIBC was higher, the grade of Fe in the concentrate was higher too. On the other hand, the presence of MIBC caused the selectivity of the process to reduce and vice versa. Table 4 shows the effect of solid content and frother type on conventional mechanical flotation results.

Table 4. Solid content effect on conventional mechanical flotation results

Description		P_2O_5 (%)		Recovery (%)	Enrichment Ratio (c/f)
Solid content (%)	Frother	Feed	Conc.		
7	Without Frother	24.77	32.49	43.1	1.31
	MIBC	24.77	29.56	85.9	1.19
25	Without Frother	24.77	31.56	64.3	1.27
	MIBC	24.77	28.76	79.4	1.16

3.1.3 Effect of aeration rate

The aeration rate is one of the applicable parameters in flotation because with the increment of air flow, the dimension of the bubbles will be increased. Therefore, in order to obtain the proper flow of aeration, the cell was evaluated for the rates of 500, 1000, 1500, 2000, and 2500 cm³/min. It should be noted that these tests were carried out on sample B. Other conditions were the same as previous experiments. The results of these tests were summarized in Table 5. It could be observed that the best results in terms of both recovery and grade were obtained with a rate of 1000 cm³/min. The process was more selective and the amount of iron removal was better in comparison to the other states.

Table 5. Effect of aeration rate on the flotation results

Air flow (cm³/min)	Concentrate		Recovery (%)	Enrichment Ratio (c/f)
	P_2O_5 (%)	Fe (%)		
500	21.97	14.87	26.33	1.62
1000	22.60	14.81	34.73	1.66
1500	21.21	15.09	23.08	1.56
2000	21.07	15.58	27.73	1.55
2500	20.93	15.62	27.54	1.54

3.2 Flotation tests result in the presence of nanobubbles in mechanical cell

3.2.1 Effect of frother on flotation results for nanobubble generation

It should be explained that in previous studies MIBC was used as a frother (Fan, 2010a; Ahmadi and Khodadadi Darban, 2013). According to the negative effect of this frother on selectivity of the process in conventional flotation, it was a concern that the usage of MIBC for the generation of nanobubbles also reduced the selectivity of the process. However, the flotation tests in the absence and presence of MIBC (100 ·10⁻⁶ g/cm³) were carried out. Considering the frothability of the collector Flo-Y-S, it seemed that it can be used as a frother for nanobubble generation. Thus, the comparison tests were conducted, and the results are illustrated in Table 6. It can be seen that the grade of P_2O_5 in the produced concentrate from Flo-Y-S (33 g/Mg), in the absence of MIBC was slightly higher than the case of using MIBC. Furthermore, although the recovery in the presence of MIBC was much higher, but the enrichment ratio showed that the selectivity of Flo-Y-S slightly better than MIBC. It is worth noting that sample A was used in these experiments.

Table 6. Effect of frother on flotation results for nanobubble generation

Frother type	P_2O_5 (%) in conc.	Yield (%)	Recovery (%)	Enrichment ratio (c/f)
MIBC	34.17	52.9	72.9	1.38
Flo-Y-S	34.76	37.9	53.1	1.40

3.2.2 Effect of charging method of frother and nanobubble solution to the cell

In these studies, the various methods of adding the frother and the solution containing nanobubbles, into the flotation cell were tested. The aim of this work was to achieve the best results of grade and recovery. MIBC was used for this purpose. In all experiments, a Denver mechanical cell with a volume of 1500 cm^3, solid content of 7%, pH of 9.5, which was adjusted by NaOH, starch as an inhibitor (400 g/Mg) and the collector Flo-Y-S with a dosage of 500 g/Mg were used. Also, the initial conditioning time, collector conditioning and frothing time were 5, 3, and 3 min, respectively. It is worth noting that nanobubbles were generated under the conditions of 350 kPa pressure, aeration flow of 200 cm^3/min, frother rate of 100 $\cdot10^{-6}$ g/cm^3 and venturi tube of 1.5 mm.

Initially, the flotation tests were performed in the presence and absence of frother (MIBC) in pure form and concentration of 100 g/m^3. Afterward, the second test was carried out under the same conditions with the difference in adding the frother. In this test, conditioning was initially done for higher solid content in one half of the cell. Then, the other half was filled with the frother solution in the absence of nanobubbles. The third test was accomplished with the same procedure, while a quarter of the cell volume (half of the mentioned solution) was from the frother solution and another half of the solution was from the nanobubble solution, which was charged directly to the cell via the nanobubble generating device. Finally, the forth test was executed, whereas 50% of the cell was filled by the nanobubble solution, which was added directly to the cell. It should be noted that these tests were done on sample B with P_2O_5 grade of 13.60%. Also, it should be considered that all of the frother solutions in these tests were added after elapsing the collector conditioning time. The above test results have been shown in Table 7. It could be found from the table that the best condition in terms of grade and recovery, occurred in the last case. This means that in the case of charging the nanobubble solution directly, in 50% of cell volume, the concentration of nanobubbles and consequently the number of nanobubbles were increased in the solution and selectively caused an increase in the recovery and grade of P_2O_5.

Table 7. Effect of charging method of frother and nanobubble solution to the cell

Flotation type	Frother charge method	P_2O_5 (%) in conc.	Yield (%)	Recovery (%)	Enrichment ratio (c/f)
Common flotation	MIBC in pure form (100 $\cdot10^{-6}$ g/cm^3)	17.28	63.7	87.7	1.38
	MIBC in solution form (100 $\cdot10^{-6}$ g/cm^3)	18.75	59.1	88.3	1.49
Presence of nanobubbles	MIBC in solution form (100 $\cdot10^{-6}$ g/cm^3): $\frac{1}{2}$ dissolved frother in solution + $\frac{1}{2}$ Nanobubble solution (25% of cell volume)	19.11	58.3	88.7	1.52
	MIBC in solution form (100 $\cdot10^{-6}$ g/cm^3): Nanobubble solution (50% of cell volume)	19.41	60.0	92.7	1.55

3.2.3 Effect of nanobubble solution to the cell volume ratio

In previous tests, it was observed that direct charging of the solution containing nanobubbles to the cell led to the best efficiency of the process. Therefore, this method was applied for the experiments in the presence of nanobubbles. However, the question is how much nanobubbles are appropriate toward cell volume and will create better conditions in terms of grade and recovery. To answer this question, flotation tests were performed with various ratios of nanobubble to cell volume. The mentioned ratios were 0, 10, 25, and 50% and the tests were done on both samples A and B. The other experimental conditions were similar. These conditions were: pH was equal to 9.5 which was prepared by NaOH, starch was applied as inhibitor at the rate of 400 g/Mg, collector Flo-Y-S dosage was 500 g/Mg and initial conditioning time as well as collector conditioning and frothing were 5, 3, and 3, respectively. Also, generation of nanobubbles occurred at a pressure of 350 kPa, aeration flow of 200 cm^3/min, and frother rate of 100 g/Mg. A venturi tube with internal diameter of 1.5 mm was used for this test.

Table 8 shows the test results. It can be seen that increment the amount of nanobubbles caused an increase in the P_2O_5 grade and decrease in the recovery. The results are shown in Figs. 7 and 8.

Table 8. Effect of nanobubble solution ratio to cell volume

Description	Nanobubbles ratio (%)	P_2O_5 (%) in conc.	Yield (%)	Recovery (%)	Enrichment ratio (c/f)
Desliming cyclone overflow	0	18.56	38.9	53.0	1.36
	10	20.35	26.3	39.3	1.50
	25	20.64	25.3	38.4	1.52
	50	22.18	23.7	38.7	1.63
Dedusting fines	0	28.19	49.9	57.1	1.17
	10	29.88	33.2	40.1	1.21
	25	31.51	26.0	32.5	1.27
	50	32.13	23.9	30.4	1.30
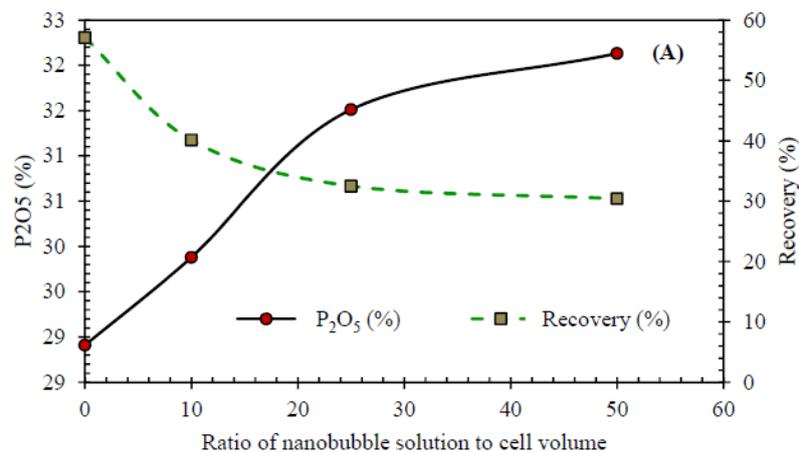
Fig. 7. Effect of nanobubble solution to cell volume ratio in flotation of crushing dusts (sample A)
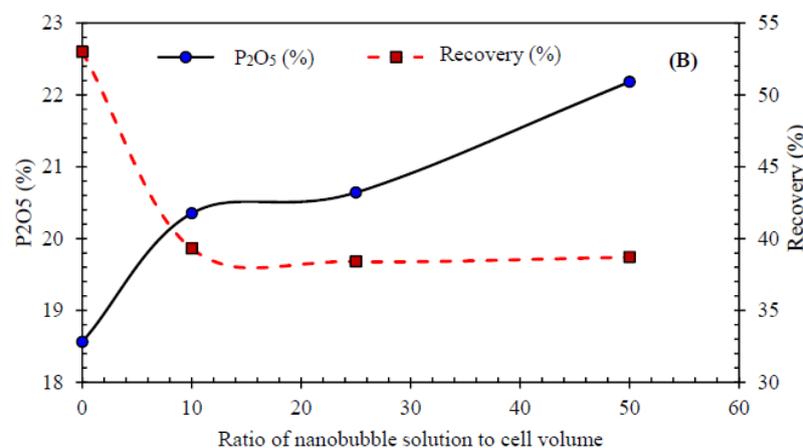
Fig. 8. Effect of nanobubble solution to cell volume ratio in flotation of desliming cyclone overflow (sample B)

3.3 Comparative tests in presence and absence of nanobubbles under optimum conditions

3.3.1 Metallurgical calculation

Due to the results of performed comparative tests based on experimental design, optimum conditions for flotation in the presence of nanobubbles were obtained at a pH of 9.5, which was provided by NaOH, starch as an inhibitor with 400 g/Mg dosage, collector Flo-Y-S at the rate of 500 g/Mg and aeration rate of 500 cm³/min. The optimized time for initial conditioning, collector preparation and frothing were obtained at 5, 3 and 3 min, respectively. Considering the frothability of Fo-Y-S and according to its best obtained results versus MIBC, it was used for generating nanobubbles with the

optimum dosage of 33 ·10⁻⁶ g/cm³ (Pourkarimi, et al., 2017) pressure of 350 kPa and aeration rate of 200 cm³/min. A venturi tube with an internal diameter of 1.5 mm was applied for this aim. The best ratio of nanobubble solution to the cell volume was determined as 50%.

Since the amount of collector consumption was equal to 500 g/Mg, considering the part of the collector that could be added with the nanobubble solution, the primary amount of collector was calculated in such a way that the total consumption was constant. Otherwise, this raises doubts that improvement of recovery is because of the collector consumption increment and not for the nanobubbles effect. Therefore, due to collector conditioning time, which was 3 min, and considering a part of the collector, which was added along with nanobubble solution, 2 min was the considered time for initial collector conditioning and the proper time for nanobubbles conditioning was considered as 1 min. In this way, the total conditioning time for the collector and frother was 3 min.

Also, the flotation tests were carried out in the absence of nanobubbles. The difference was due to the absence of nanobubbles in the process, and the collector with the amount of 500 g/Mg was added to the cells at the same time. It should be noted that these experiments were conducted on crushed fine dusts (sample A) as rougher tests. It is noteworthy that the results of the same tests on the desliming overflow fine particles (sample B) showed that the results were accessible by two stages of flotation as rougher and cleaner tests. Evaluating the chemical analysis of the feed sample (crushing dusts) and the flotation product in the presence and absence of nanobubbles it was shown that the existence of nanobubbles in the process had positive effects, therefore more than 90% of the phosphate content, with a grade of more than 40% was recoverable in the presence of nanobubbles, and in the absence of nanobubbles, under the same conditions, a grade of P_2O_5 reached 37%. The flotation recovery of apatite in the presence of nanobubbles had a significant increment of more than 30, versus flotation in the absence of nanobubbles which was a unique result in flotation of fine particles. The recovery of light rare earth elements such as Ce, La and Nd in the presence of nanobubbles was higher than the concentrate of conventional flotation in the absence of nanobubbles which was very desirable, as well as Fe and SiO_2 which were tailings. The recovery was lower in the concentrate produced the presence of nanobubbles toward the conventional method, which indicated the selectivity of the process. Table 9 presents the comparison of grade and recovery after flotation in the presence and absence of nanobubbles.

The best results of flotation tests were obtained in smaller sizes of nanobubbles. Furthermore, using the collector FLO-Y-S instead of MIBC as a frother, which has more frothability property (Pourkarimi, 2017), generation of nanobubbles causes the results to become better and more selective.

In a normal air flow rate of 500 and 1000 cm³/min and combining with nanobubbles, in dimensions (d_{50}) smaller than 150 nm, the recovery increased up to more than 30% versus the conventional flotation method.

Table 9. Comparing the results of flotation in presence and absence of nanobubbles

Sample/compound	Unit	Initial feed-crushed dusts	Flotation concentrate, with nanobubbles		Conventional flotation concentrate, without nanobubbles	
		Grade (%)	Grade (%)	Recovery of P_2O_5 (%)	Grade (%)	Recovery of P_2O_5 (%)
P_2O_5	(%)	24.77	40.38		37.01	
Fe_{Total}	(%)	16.43	4.25		6.28	
SiO_2	(%)	9.34	6.29	70.2	7.05	34.8
Ce	(ppm)	5814	7799		6763	
La	(ppm)	2444	3305		2853	
Nd	(ppm)	1938	2593		2229	

3.3.2 Comparing size of flotation products

The size of flotation concentrate in the presence and absence of nanobubbles was evaluated by the laser particle size analyzer (LPSA), and the result are shown in Table 10. It can be found that from the comparison of the d_{10}, d_{50}, and d_{90}, the concentrate of two products of flotation in the presence of

nanobubbles had smaller dimensions toward the conventional flotation concentrate. On the other hand, using nanobubbles in flotation increased the chance of finer particles to be floated.

Table 10. Comparing product size of flotation in presence and absence of nanobubbles

Sample/size	Initial feed-crushed dusts	Flotation concentrate in the presence of nanobubbles	Conventional flotation concentrate in the absence of nanobubbles
d_{10} (μm)	2.19	2.03	2.05
d_{50} (μm)	15.03	15.2	16.17
d_{90} (μm)	37.12	37.48	39.13

4. Conclusions

Generation of nanobubbles was performed by a special device, which was manufactured at IMPRC. The base of nanobubbles in this device was hydrodynamic cavitation, which was supplied by a 1.5 mm-venturi tube.

Flo-Y-S, which is a fatty acid collector considering its frothability, was used for concentrating the apatite. According to our knowledge, considering previous similar works, it was the first time that a collector was used for nanobubble generation by the cavitation technique. The generated nanobubbles by Flo-Y-S were significantly smaller than those produced by MIBC.

The best conditions for generating nanobubbles were obtained as follows: pressure of 350 kPa, aeration flow of 200 cm³/min, frother rate of $33 \cdot 10^{-6}$ g/cm³ Flo-Y-S, and venturi tube with internal diameter of 1.5 mm.

Higher amounts of nanobubbles in the cell led to more recovery increment. Moreover, the best results of flotation tests were obtained in smaller sizes of nanobubbles. Furthermore, using the collector FLO-Y-S instead of MIBC as a frother, which has more frothability property in the generation of nanobubbles, led to better and more selective results.

In a normal air flowrate of 500 and 1000 cm³/min and combined with nanobubbles, in dimensions (d_{50}) smaller than 150 nm, the recovery increased up to more than 30%, in comparison with the conventional flotation method. Interestingly, the mentioned recovery for sample A was obtained in one stage of the rougher flotation. It should be noted that the same result was accessible for sample B by two stages of flotation as rougher and cleaner.

Evaluating the chemical analysis of the feed sample and flotation products in the presence and absence of nanobubbles showed that the existence of nanobubbles in the process had positive effects, so that more than 90% of phosphate, with a grade of more than 40% was recoverable in the presence of nanobubbles, while in the absence of nanobubbles, under the same conditions, a grade of P_2O_5 was 37%. The recovery of apatite in flotation in the presence of nanobubble, significantly increased up to more than 30% in comparison to flotation in the absence of nanobubbles which is a unique result in the flotation of fine particles.

The recovery of light rare earth elements such as Ce, La and Nd in the presence of nanobubbles was higher than in the conventional flotation in the absence of nanobubbles, which is very desirable. Also Fe and SiO_2 had lower amounts in the flotation concentrate produced in the presence of nanobubbles.

The size of flotation concentrate particles in the presence and absence of nanobubbles was evaluated by laser particle size analyzer (LPSA). It was found from a comparison of two curves of the products, that the concentrate of flotation in the presence of nanobubbles had smaller dimensions toward the conventional flotation concentrate. On the other hand, using nanobubbles in flotation increased the chance of finer particle flotation.

Reference

AHMADI R., KHODADADI DARBAN A., 2013. *Modelling and optimization of nano-bubble generation process using response surface methodology*. International Journal of Nanoscience and Nanotechnololgy, 9(3), 151-162.

ANFRUS J.F., KITCHENER J.A., 1977. *Rate of capture of small particles in flotation*. Transactions of the Institution of Mining and Metallurgy, Section C: Mineral Processing and Extractive Metallurgy, 86, 9-15.

COLIC M., MORSE W., MILLER J.D., 2007. *The development and application of centrifugal flotation systems in waste water treatment*. International Journal of Environment and Pollution, 30(2), 296-312.

CRUZ N., PENG Y., FARROKHPAY S. & BRADSHAW D., 2013. *Interactions of clay minerals in copper–gold flotation: Part 1–Rheological properties of clay mineral suspensions in the presence of flotation reagents*. Minerals Engineering, 50, 30-37.

DERJAGUIN B.V., DUKHIN S.S., 1961. *Theory of flotation of small and medium-size particles.* Progress in Surface Science, 43, 241-266.

DERJAGUIN B.V., DUKHIN S., RULYOV N., 1984. *Kinetic theory of flotation of small particles*. Surface and Colloid Science, 13, 71–113.

FAN M., 2008. *Picobubble enhanced flotation of coarse phosphate particles*. Ph.D. Dissertation in Mineral Processing, University of Kentucky, Kentucky, USA.

FAN M., TAO D., 2008. *A study on picobubble enhanced coarse phosphate froth flotation*. Separation Science and Technology, 43, 1-10.

FAN M., TAO D., HONAKER R., LUO Z., 2010a. *Nanobubble generation and its application in froth flotation (Part I): Nanobubble generation and its effects on properties of microbubble and millimeter scale bubble solutions*. Mining Science and Technology, 20, 1–19.

FAN M., TAO D., HONAKER R., LUO Z., 2010b. *Nanobubble generation and its applications in froth flotation (Part II): Fundamental study and theoretical analysis*. Mining Science and Technology, 20, 159-177.

FAN M., TAO D., HONAKER R., LUO Z., 2010c. *Nanobubble generation and its applications in froth flotation (Part III): Specially designed laboratory scale column flotation of phosphate*. Mining Science and Technology, 20(3), 317-338.

FAN M., TAO D., HONAKER R., LUO Z., 2010d. *Nanobubble generation and its applications in froth flotation (Part IV): Mechanical cells and specially designed column flotation of coal*. Mining Science and Technology, 20, 641-671.

GAUDIN A.M., SCHUHMANN J.R., SCHLECHTEN A.W., 1942. *Flotation kinetics II. The effect of size on the behaviour of galena particles*. Journal of Physical Chemistry, 46, 902–910.

HAMPTON M.A., NGUYEN A.V., 2010. *Nanobubbles and the nanobubble bridging capillary force*. Advances in Colloid and Interface Science, 154, 30–55.

ISO 13320, 2009. *Particle size analysis-laser diffraction methods, Part 1*. General principals.

KAISAR ALAM, S. M., 2012. *Electroflotation: its application to water treatment and mineral processing*. Research Doctorate - Doctor of Philosophy (PhD), University of Newcastle, Faculty of Engineering and Built Environment, School of Engineering.

MIETTINEN T., RALSTON J., FORNASIERO D., 2010. *The limits of fine particle flotation*. Minerals Engineering, 23, 420–437.

MOHANTY M.K., HONAKER R.Q., 1999. *Performance optimization of Jameson flotation technology for fine coal cleaning*. Minerals Engineering, 12(4), 367-381.

NGUYEN A.V., GEORGE P., JAMESON G.J., 2006. *Demonstration of a minimum in the recovery of nanoparticles by flotation: Theory and experiment*. Chemical Engineering Science, (8), 2494–2509.

POURKARIMI Z., REZAI B., NOAPARAST M., 2017. *Effective parameters on generation of nanobubbles by cavitation method for froth flotation applications*. Physicochemical Problems of Mineral Processing, 53(2), 920−942.

REAY D., RATCLIFF G.A., 1973. *Removal of fine particles from water by dispersed air flotation. Effects of bubble size and particle size on collection efficiency*. Canadian Journal of Chemical Engineering, 51, 178–185.

RODRIGUES R.T., RUBIO J., 2007. *DAF–dissolved air flotation: Potential applications in the mining and mineral processing industry*. Int. J. Miner. Process, 82, 1-13.

SADOWSKI Z., POLOWCZYK I., 2004. *Agglomerate flotation of fine oxide particles*. International Journal of Mineral Processing, 74(1–4), 85–90.

SHAFAEI TONEKABONI Z., 2006. *Evaluation of fine particles separation from Esfordi phosphate plant feed before rod mill for optimizing the comminution circuit*. IMPASCO, (in Persian).

SIVAMOHAN R., 1990. *The problem of recovering very fine particles in mineral processing – A review*. International Journal of Mineral Processing, 28(3-4), 247-288.

SOBHY A., TAO D., 2013. *Nanobubble column flotation of fine coal particles and associated fundamentals*. International Journal of Mineral Processing, 124, 109-116.

SUTHERLAND K. L., 1948. *Physical Chemistry of Flotation. XI. Kinetics of the Flotation Process*. J. Phys. Chem., 52 (2), 394–425.

TAO D., 2004. *Role of bubble size in flotation of coarse and fine particles-a review*. Separation Science and Technology, 39, 741-760.

TAVAKOLI A., 2007. *Technical Archive of Esfordi phosphate complex*.

TASDEMIR A, TASDEMIR T. and OTEYAKA B., 2007. *The effect of particle size and some operating parameters in the separation tank and the downcomer on the Jameson cell recovery*. Minerals Engineering, 20, 1221-1336.

TASDEMIR A, TASDEMIR T. and GECGEL Y., 2011. *Removal of fine particles from wastewater using induced air flotation*. The Online Journal of Science and Technology, 1(3).

YOON R. H., 2000. *The role of hydrodynamic and surface forces in bubble-particle interaction*. International Journal of Mineral Processing, 58, 129-143.

ZHANG M, SEDDON J.R., 2016. *Nanobubble–nanoparticle interactions in bulk solutions*. Langmuir, 32(43), 11280-11286.

ZHOU Z.A., XU Z., FINCH J.A., MASLIYAH J.H., CHOW R.S., 2009. *On the role of cavitation in particle collection in flotation –A critical review. II*. Minerals Engineering, 22, 419–433.

ZHOU Z.A., XU Z., FINCH J.A., 1994. *On The role of cavitation in particle collection during flotation- A critical review*. Minerals Engineering, 7(9), 1073-1084.